

## **A New Calibration Method for Binocular Camera Based on Fundamental Matrix & HEIV Model**

Hui Ma

Jilin Agricultural Science and Technology University, Jilin 132109, China

(mahuiaini8@163.com)

### **Abstract**

With the fast development of geometrics' industry, the implementation of digital city and digital earth strategy has become an important step for information construction. The 3D spatial data are the foundation and precondition for establishing digital earth and intelligent city. The binocular vision technology mainly comprising the steps of image acquisition, stereo matching, and 3D reconstruction can obtain geographic information quickly. Binocular camera calibration is an essential step to obtain 3D information from images. In this paper, a new 1D calibration method was proposed based on fundamental matrix. In this calibration method, 1D Object can move freely without any limitations, such as the space or prior information of the camera. Then a HEIV (Heteroscedastic Error-in-Variables) model was proposed to improve the calibration accuracy. Both simulation experiment and real image experiment were conducted to validate the feasibility and effectiveness of this algorithm.

### **Keywords**

Geographic information, Binocular camera calibration, Fundamental matrix, HEIV model.

### **1. Introduction**

The binocular camera imaging technology has developed rapidly in recent years, especially in the field of geometrics' industry. Binocular camera calibration is an essential step to obtain 3D information from images. Generally speaking, binocular camera calibration is mainly targeted at two internal parameters (focal length and the optical center) of the camera and the external parameters (relative position of each camera). Current calibration methods include 3D calibration

method, 2D calibration method [1], 1D calibration method and 0D calibration method [2]. Since the 1D calibration accuracy is higher than the 0D calibration accuracy, and 1D calibration object is simpler and more portable compared with the 2D and 3D calibration objects, the 1D calibration method has received widespread attention since it was first put forward by Zhang in 2004 [3]. However, in Zhang's and many of the relevant methods of 1D calibration, an endpoint of the calibration object must be fixed. On this basis, the 1D calibration object can only move in a specific space or needs the prior knowledge of the camera parameters [4], which strongly limited the rigid motion of the calibration object.

Given this problem, a one-dimensional calibration method was proposed based on the fundamental matrix. In this method, 1D calibration object can move arbitrarily, without calculating the vanishing point and any prior knowledge. Then, HEIV (Heteroscedastic Error-in-Variables) model was proposed to optimize the data, thus improving the calibration accuracy. The proposed algorithm considered that all data were affected by noises, and minimized the sum of errors between the contaminated data and the estimated data iteratively. After continuous iteration, this algorithm significantly increases the accuracy of data.

## 2. Camera Geometric Model and HEIV Model

### 2.1 Geometric Model of Binocular Camera

Assume that a 3D point was represented by  $M = [X, Y, Z]^T$ , the homogeneous coordinate was represented by  $\tilde{M} = [X, Y, Z, 1]^T$ , and a 2D point was represented by  $m = [u, v]^T$ ,  $\tilde{m}$  as homogeneous coordinate (similarly hereinafter). The relationship between  $M$  and  $m$  is shown as below:

$$s\tilde{m} = K[R, t]\tilde{M}K = \begin{bmatrix} \alpha & \gamma & \mu \\ 0 & \beta & \nu \\ 0 & 0 & 1 \end{bmatrix} \quad (1)$$

$S$  is a scale factor,  $P = K[R, t]$  is camera matrix,  $K$  is intrinsic matrix,  $R$  is rotation matrix, and  $t$  is translation vector.  $\alpha, \beta$  are scale factors,  $[\mu, \nu]$  is the main point of the camera, and  $\gamma$  is the inclination factor. So, the calculation of the camera matrix  $P$  is the core of camera calibration. Usually the world coordinate system coincided with the left camera coordinate system. The following equation is obtained:

$$\begin{cases} \widetilde{m}_1 = s_1 K_1 [I, 0] \widetilde{M}_1 \\ \widetilde{m}_2 = s_2 K_2 [R, t] \widetilde{M}_2 \end{cases} \quad (2)$$

## 2.2 1D Calibration Object

Assume that 1D calibration object consists three points A, B and C. The Euclidean distance between each point is known. Details are shown in figure 1. Within the vision scope of the binocular cameras, move 1D calibration object freely for many times, to complete the camera calibration.

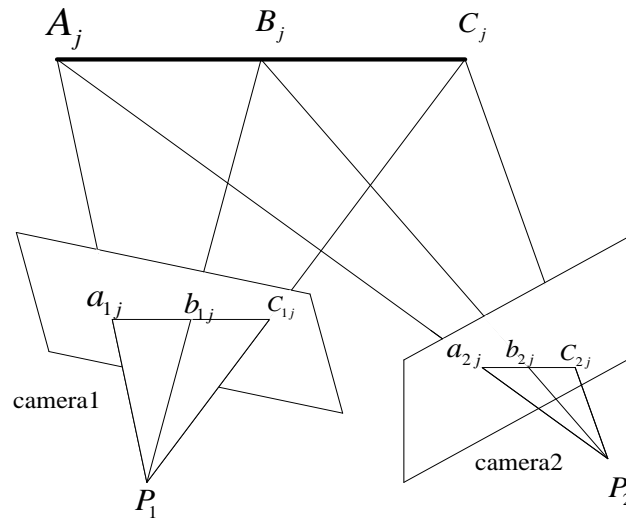


Fig.1. Calibration sketch for binocular camera using a 1D calibration object

## 2.3 HEIV Model

HEIV (heteroscedastic Error-in-Variables) model was used to solve the problem of optimal estimation of parameters, which is affected by noise. Generally, assume  $u_j$  as the  $j^{\text{th}}$  actual measurement data. And there is some deviation between the measurement data affected by the noise and the true value.  $u_j$  is defined as:

$$u_j = \bar{u}_j + \delta u_j, \delta u_j \sim \text{GI}(\mu, C_{u_j}), j = 1, 2, \dots, n \quad (3)$$

Where  $\bar{u}_j$  is the true value of the measurements,  $\delta u_j$  is the measuring error,  $\delta u_j \sim \text{GI}(\mu, C_{u_j})$  stands for independent probability density with mean  $\mu$  and covariance  $C_{u_j}$ . The constraint between the true value of the measurements and the true value of estimator satisfies:

$$\varphi(\bar{u}_j, \bar{\beta}) = 0, j = 1, 2, \dots, n \quad (4)$$

The Eq. (4) can be decomposed into two parts, namely, the measurement data matrix  $\Phi(\bar{u}_j)$  and estimated parameter vector  $\Theta(\bar{\beta})$  (Matei and Meer, 2006):

$$\varphi(\bar{u}_j, \bar{\beta}) = \Phi(\bar{u}_j)\Theta(\bar{\beta}) = 0 \quad (5)$$

By the transformation of (5), true value measurements can be separated from Eq. (4) to reduce the calculation difficulty of the problem. On the other hand, the estimated parameters can be represented as n-dimensional vector.

### 3. Fundamental Matrix Algorithm

The fundamental matrix is a 3x3 matrix, which represents the correspondence of the image point coordinate on each binocular camera. The relationship is as follows:

$$a_1^T F a_2 = 0 \quad (6)$$

Where  $a_1 a_2$  is the image point coordinate on each binocular camera.

Move the 1D calibration object containing three feature points for more than five times, and then use the projection around the camera's image point coordinate. Calculate the camera fundamental matrix F through the modified eight point-based method [5]

Fundamental matrix F was used to calculate the projection matrix P of left and right camera. The projection matrix P of the two cameras satisfied [6]:

$$\begin{cases} P_1 = [I, 0] \\ P_2 = [[\tilde{e}]_{\times} F, \tilde{e}] \end{cases} \quad (7)$$

Where e is the epipole of the right camera,  $[\tilde{e}]_{\times}$  is the antisymmetric matrix defined by the homogeneous vector of point e and I is a 3x3 identity matrix.

The relationship between the projection matrix and camera matrix under the Euclidean space satisfies [7]:

$$\bar{P}_1 = H P_1, \bar{P}_2 = H P_2 \quad (8)$$

Where  $\bar{P}_1, \bar{P}_2$  are the two cameras' matrices in Euclidean space. H is denoted by:

$$H = a \begin{bmatrix} K_1^{-1} & 0 \\ Q^T & q \end{bmatrix} \quad (9)$$

Where H is a 4x4 matrix, and  $K_1$  is the intrinsic matrix of the left camera. Assume that:

$$W = a[Q^T, q] \quad (10)$$

Where W is a four-dimensional vector coordinate. The key of the problem is to calculate H and W by the geometrical constraint conditions of one-dimensional calibration. The relationship of the point between the Projected Coordinate System and Euclidean Coordinate System satisfies [7]:

$$\tilde{A}_j = H\tilde{A}_j \quad \tilde{B}_j = H\tilde{B}_j \quad \tilde{C}_j = H\tilde{C}_j \quad (11)$$

As shown in Figure1,  $\tilde{A}_j, \tilde{B}_j, \tilde{C}_j$  are three feature points on the 1D calibration object; j is the j<sup>th</sup> movement in Euclidean Coordinate System.

The relationship between the object point coordinate in the Projected Coordinate System and image point coordinate satisfies [8]:

$$\begin{cases} \tilde{a}_{1j} = P_1\tilde{A}_j, \tilde{b}_{1j} = P_1\tilde{B}_j, \tilde{c}_{1j} = P_1\tilde{C}_j \\ \tilde{a}_{2j} = P_2\tilde{A}_j, \tilde{b}_{2j} = P_2\tilde{B}_j, \tilde{c}_{2j} = P_2\tilde{C}_j \end{cases} \quad (12)$$

Where  $\tilde{a}_{1j}, \tilde{a}_{2j}$  are the measurements. The object point coordinate in the Projected Coordinate System can be calculated via (12).

$\bar{A}_j, \bar{B}_j, \bar{C}_j$  the three feature points satisfy:

$$\bar{B}_j = d_1\bar{A}_j + d_2\bar{C}_j \quad (13)$$

Where  $d_1, d_2$  are the distance scale factors. Assume that  $\|A_j - C_j\| = L, \|B_j - C_j\| = L_1$ , and it is concluded that  $d_1 = (L - L_1)/L, d_2 = L_1/L$ , which are the measurements.

By substituting (9) (11) into (13), the following equation is obtained:

$$\frac{1}{\bar{B}_j^T W} B_j = \frac{d_1}{\bar{A}_j^T W} A_j + \frac{d_2}{\bar{C}_j^T W} C_j \quad (14)$$

The cross product  $B_j$  on both sides of the equation is as follows:

$$\frac{d_1}{\bar{A}_j^T W} (A_j \times B_j) + \frac{d_2}{\bar{C}_j^T W} (C_j \times B_j) = 0 \quad (15)$$

Then the dot product  $(C_j \times B_j)$  on both sides of the equation is:

$$\left[ \bar{A}_j + \frac{d_1(A_j \times B_j)(C_j \times B_j)}{d_2(C_j \times B_j)(C_j \times B_j)} \bar{C}_j \right] W = 0 \quad (16)$$

According to the Eq. (10),  $W$  is a four dimensional vector coordinate which is not affected by the movement of the 1D object, so we can compute  $W$  with the 1D calibration object which moved over 3 times.

The next step is to calculate the  $a$  and  $K_1$  in (9). The depth of the relationship between the image point coordinates of the left camera and the point coordinates of the object in Euclidean space satisfies:

$$\begin{cases} \bar{A}_j = Z_j^a K_1^{-1} \tilde{a}_{1j} \\ \bar{B}_j = Z_j^b K_1^{-1} \tilde{b}_{1j} \\ \bar{C}_j = Z_j^c K_1^{-1} \tilde{c}_{1j} \end{cases} \quad (17)$$

By substituting (17) into the (14), we have:

$$\begin{cases} Z_j^a = \frac{aA_j}{\bar{A}_j^T W \tilde{a}_{1j}} \\ Z_j^b = \frac{aB_j}{\bar{B}_j^T W \tilde{b}_{1j}} \\ Z_j^c = \frac{aC_j}{\bar{C}_j^T W \tilde{c}_{1j}} \end{cases} \quad (18)$$

The distance between the three point which can be measured in Euclidean space satisfies:

$$\begin{cases} \|\bar{B}_j - \bar{A}_j\| = d_3 \\ \|\bar{C}_j - \bar{B}_j\| = d_4 \end{cases} \quad (19)$$

By substituting (17) (18) into (19), we have:

$$\begin{cases} \left\| aK_1^{-1} \left( \frac{B_j}{\tilde{B}_j^T W} - \frac{A_j}{\tilde{A}_j^T W} \right) \right\| = d_3 \\ \left\| aK_1^{-1} \left( \frac{C_j}{\tilde{C}_j^T W} - \frac{B_j}{\tilde{B}_j^T W} \right) \right\| = d_4 \end{cases} \quad (20)$$

The former equations are equivalent to:

$$\begin{cases} g_j^T N g_j = d_3^2 \\ q_j^T N q_j = d_4^2 \end{cases} \quad (21)$$

Where  $g_j = \left( \frac{B_j}{\tilde{B}_j^T W} - \frac{A_j}{\tilde{A}_j^T W} \right)$ ,  $q_j = \left( \frac{C_j}{\tilde{C}_j^T W} - \frac{B_j}{\tilde{B}_j^T W} \right)$ ,  $N = a^2 K_1^{-T} K_1^{-1}$ ,  $N$  is a 3\*3 symmetric matrix.

From (21), a set of matrix equation group was obtained:

$$D_j n = d' \quad (22)$$

Where  $n = [n_{11}, n_{12}, n_{22}, n_{13}, n_{23}, n_{33}]$ , with  $n_{xy}$  equaling to the element of the x-th row and y-th column of  $N$ .  $d' = [d_3^2, d_4^2]^T$  and  $D_j$  is a 2\*6 matrix, whose elements are dependent on the vectors  $g_j$  and  $q_j$ .

So, we can compute  $aK_1^{-1}$  by moving 1D calibration object for over 5 times. Finally, the parameter  $K$  can be calculated by the Cholesky decomposition.

#### 4. HEIV-Based 1D Calibration Algorithm

In fact, all variables are affected by noises. The calibration parameters were optimized by HEIV algorithm, which can optimize the sum of errors between the contaminated data and the estimated data iteratively.

Eq. (16) can be transformed as follows:

$$V_j = \left[ \tilde{A}_j + \frac{d_1(A_j \times B_j)(C_j \times B_j)}{d_2(C_j \times B_j)(C_j \times B_j)} \tilde{C}_j \right] \text{ then, } \varphi = V_j W = 0 \quad (23)$$

Since Eq. (23) is similar to (5), the problem of computing  $W$  can be treated as HEIV model. Mahalanobis distance is a kind of statistical distance measurement, which can fully express the distribution characteristics of the image noises. Thus, Markov distance is suitable for the error calculation, and the cost function satisfies:

$$J = \frac{1}{2} \sum_{j=1}^N (u_j - u'_j)^T C_{u_j}^- (u_j - u'_j) \quad (24)$$

Where  $u_j = [A_{j1} \ A_{j2} \ B_{j1} \ B_{j2} \ C_{j1} \ C_{j2}]$  are the measurements;  $A_{j1}$  and  $A_{j2}$  are the coordinate components in the Projected Coordinate System;  $C_{u_j} = \sigma^2 I_6$  is the covariance matrix of  $u_j$ .

Considering Eq. (23), the parameter  $W$  can be calculated by optimizing the cost function as follows:

$$J_s = J + \sum_{j=1}^N \eta_j \varphi \quad (25)$$

Where  $\eta_j$  is the Lagrangian multiplier. The estimated parameter  $W$  satisfies:

$$\frac{\partial J_s}{\partial u'_j} = 0 \quad (26)$$

$$\frac{\partial J_s}{\partial W'} = 0 \quad (27)$$

With Eq. (26), the following equation is obtained:

$$C_{u_j}^- (u_j - u'_j) = \frac{\partial \varphi}{\partial u'_j} \eta_j \quad (28)$$

With Eq. (28), then:

$$u'_j = u_j - C_{u_j} \frac{\partial \varphi}{\partial u'_j} \eta_j \quad (29)$$

With Eq. (26)(28)(29), the Lagrangian multiplier  $\eta_j$  satisfies:

$$\eta_j = C_{\varphi}^+ \varphi \quad (30)$$

Where  $C_\varphi = \left(\frac{\partial\varphi}{\partial u_j'}\right)^T C_{u_j} \frac{\partial\varphi}{\partial u_j'}$ , and  $C_\varphi^+$  is the pseudo-inverse.

Likewise, from Eq. (27), the following equation is obtained:

$$\frac{\partial J_s}{\partial W'} = (S_W - C_W)W = 0 \quad (31)$$

The scatter matrix satisfies:

$$S_W = \sum_{j=1}^N \Phi^T C_{\varphi(u_j)}^+ \Phi \quad (32)$$

Where  $\Phi = [V_j \ 1]$ .

The weighted covariance matrix satisfies:

$$C_W = \sum_{j=1}^N (\eta_j^T \otimes I_7) C_{\varphi(u_j)} (\eta_j \otimes I_7) \quad (33)$$

Where  $\phi(u_j) = \text{vec}\Phi^T$ , meaning that a row vector is generated by Matrix  $\Phi$  in accordance with the order of the column vectors.  $\otimes$  is the Kronecker product.

Finally, detailed steps of this algorithm are given as follows:

- (1) Calculate the initial values of  $V_j$ ,  $W$  and  $C_{\varphi(u_j)}$  by Eq. (16).
- (2) Calculate the scatter matrix  $S_W$  and the weighted covariance matrix  $C_W$  with Eq. (32) and (33), then construct the generalized eigenvalue problem:

$$S_W W = \lambda C_W W \quad (34)$$

(3) Update parameters. Compute new  $W'$  with Eq. (34). Update the estimated measurements  $u_j'$  with Eq. (29) and the estimated  $V_j$  with Eq. (16).

(4) Back to step 2 until the smallest eigenvalue  $\lambda = 1$  in Eq. (34).

(5) Calculate  $aK_1^{-1}$  with Eq. (17,18,19,20,21,22). Finally compute  $K$  by the Cholesky decomposition.

## 5. Experimental Results

### 5.1 Simulation Experiment

The left camera simulation parameters are as follows:  $\alpha = \beta = 1000$ ,  $[\mu, \nu] = [512, 384]$ ,  $\gamma = 0$ . The right camera simulation parameters are as follows:  $\alpha = \beta = 1100$ ,  $[\mu, \nu] = [512, 384]$ ,  $\gamma = 2$ . Each image point added Gaussian noise with mean 0 and variance  $\sigma^2$ . The noise level varied from 0 to 1.2 pixels with a step of 0.15 pixels. Do 200 times test for each noise level to make the results more statistically meaningful. To make comparisons, the RMS errors between the results of the HEIV and those based on the fundamental matrix algorithms are computed. Results were shown in Figure 2 and Figure 3.

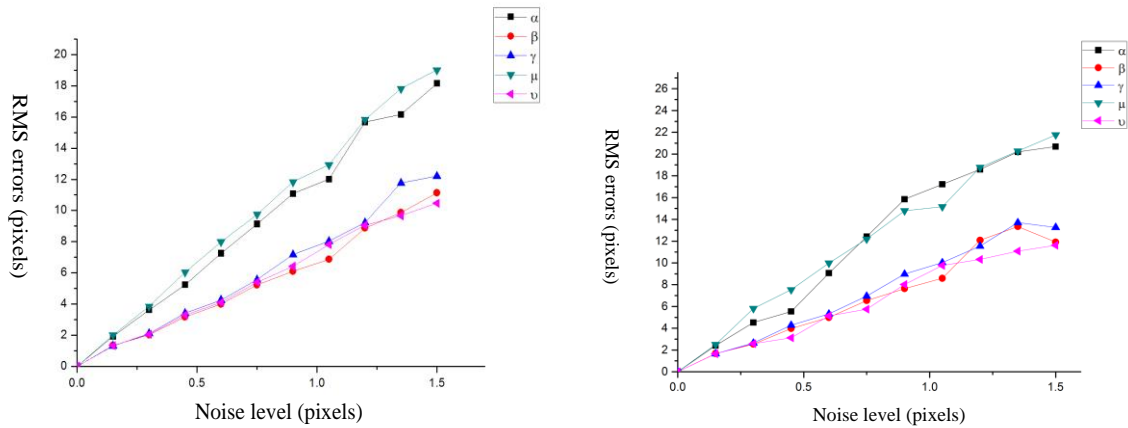


Fig.2. The RMS errors of the fundamental matrix algorithm

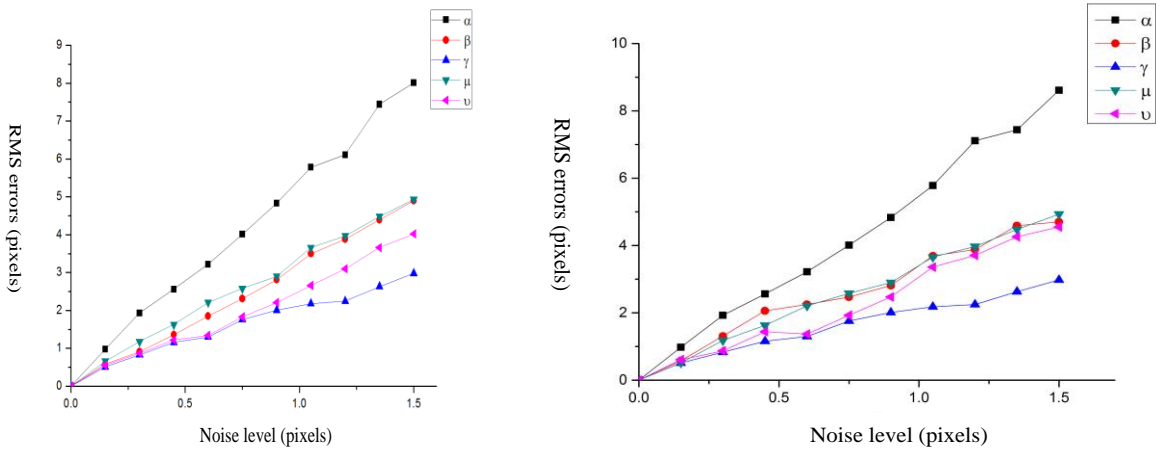


Fig.3. The RMS errors of the HEIV algorithm

Synthetic data experiment results show that, the HEIV algorithm is obviously consistently superior to the fundamental matrix algorithm. With the increase of noise, the noise suppression effect is obvious by HEIV algorithm. Both algorithms are almost not affected by the radial distortion.

## 5.2 Real Image Experiment



Fig.4. 1D object in experiment

This experiment adopts CCD binocular camera of Microvision Inc., with the model of MV-VS220 and resolution of 1280x960.

The 1D object is a stick with three feature points. The distance between the adjacent two points is 15cm. Details are shown in Figure4.

Move the one dimensional calibration object for 20 times, then use the fundamental matrix algorithm and HEIV to calibrate the camera. Since the coordinates of such correspondences are obtained accurately, the fundamental matrix  $F$  will be calculated. Details are shown in Eq. (35). We also adopt Zhang's 2D algorithm to calibrate the camera. And the results of Zhang's 2D algorithm serve as the real value for comparison. Calibration data of each algorithm was shown in figure 1.

$$F = \begin{bmatrix} -3.620471e - 009 & -4.119046e - 007 & 1.400931e - 004 \\ 1.224463e - 006 & 3.395123e - 009 & 1.579353e - 002 \\ -5.141536e - 004 & -1.683020e - 002 & 1.000000e + 000 \end{bmatrix} \quad (35)$$

left camera	fundamental matrix algorithm	3224.5	3245.1	2.3216	619.46	484.09
	HEIV algorithm	3359.6	3331.1	1.2235	637.48	515.16
	Zhang's 2D algorithm	3476.2	3479.5	0.669	662.33	533.54
right camera	fundamental matrix algorithm	3648.5	3719.1	-3.3603	712.36	547.32
	HEIV algorithm	3580.8	3637.6	-1.7325	693.02	534.29
	Zhang's 2D algorithm	3476.6	3480.7	-1.0545	667.37	509.31

Fig.5. Results of real image experiment

The results indicate that calibration precision of HEIV algorithm is matched with Zhang's 2D algorithm. And the HEIV algorithm is prior to the fundamental matrix algorithm.

## Conclusions

This paper proposed a 1D calibration method based on the fundamental matrix. In this method, one dimensional calibration object can move arbitrarily without any prior information of the cameras or motion. Then an HEIV optimization algorithm was proposed. The algorithm can greatly improve the calibration accuracy compared with previous algorithms. The method is suitable for outdoor real-time calibration. Both Simulation experiment and real image experiment validate the feasibility and effectiveness of this algorithm.

## References

1. R. Tsai, An efficient and accurate camera calibration technique for 3d machine vision, 1986, ROC IEEE Conf. on Computer Vision & Pattern Recognition, pp. 364–374.
2. K.F. Shi, F.C. Wu, Optimally weighted linear algorithm for camera calibration with 1D object, 2014, Journal of Computer-Aided Design & Computer Graphics, vol. 26, no. 8, pp. 1251-1257.
3. Z.Y. Zhang, Camera calibration with one- dimensional objects, 2004, European Conference on Computer Vision, Vol. 26, no. 7, pp. 892-899.
4. W.W. Wang, W. Yang, J. Luo, A new calibration method of camera external parameters, 2014, Semiconductor optoelectronics, vol. 35, no. 6, pp. 1127-1130.
5. X. Armangue, J. Salvi, Overall view regarding fundamental matrix estimation, 2003, Image and Vision Computing, vol. 21, no. 2, pp. 205–220.
6. O.D. Faugeras, What can be seen in three dimensions with an uncalibrated stereo rig, 1992, European Conference on Computer Vision, pp. 563–578.
7. R. Hartley, A. Zisserman, Multiple View Geometry in Computer Vision, 2000, Cambridge University Press.
8. M. Pollefeys, L.V. Gool, A Oosterlinck. The modulus constraint: a new constraint for self-calibration, 1996, Proc of the ICPR'96 Vienna Austria, pp. 31-42.
9. J. Franca, M.R. Stemmer, Revisiting zhang's 1d calibration algorithm, Pattern Recognition, vol. 43, no. 3, pp. 1180–1187.
10. Q. Fu, Q. Quan, K.Y. Cai, Calibration method and experiments of multi-camera's parameters based on freely moving one-dimensional calibration object, 2014, Control Theory & Applications, vol. 31, no. 8, pp. 1018-1024.
11. G.H. Golub, C.F. Van Loan, Matrix Computations, 1996, The Johns University Press.

12. R. Horaud, G. Csurka, D. Demirdijian, Stereo calibration from rigid motions, 2000, IEEE Transactions on Pattern Analysis and Machine Intelligence, vol. 22, no. 12, pp. 1446–1452.
13. L. Li, Camera calibration algorithm based on OpenCV and improved Zhang Zhengyou Algorithm, 2015, Light Industry Machinery, vol. 33, no. 4, pp. 60-68.
14. B.C. Matei, P. Meer, Estimation of nonlinear errors-in-variables models for computer vision application, 2006, IEEE Transactions on Pattern Analysis and Machine Intelligence, Pattern Recognition, vol. 28, no. 10, pp. 1537–1552.
15. I. Miyagawa, H. Arai, H. Koike, Simple camera calibration from a single image using five points on two orthogonal 1-D objects, 2010, IEEE Trans Image Processing, vol. 19, no 6, pp. 1528-1538.
16. L. Wang, F.C. Wu, Z.Y. Hu, Multi-camera calibration with one-dimensional object under general motions, 2007, Proc of the ICCV' 07 IEEE, pp. 1-7.
17. Z.Y. Zhang, A flexible new technique for camera calibration, 2000, IEEE Transactions on Pattern Analysis & Machine Intelligence, vol. 22, no. 11, pp. 1330–1334.
18. Z.J. Zhao, Y.C. Liu, Z.Y. Zhang, Camera calibration with three noncollinear points under special motions, 2008, IEEE Trans. Image Processing, Vol. 17, no. 12, pp. 2393-2402.
19. D. Zhou, L.Q. Zhou, J. Sun, A novel feedback error-correcting algorithm for automatic recognition of the color and weave pattern of yarn-dyed fabrics, 2015, Textile Research Journal, Vol. 83 no. 16, pp. 1673-1689.